Compressive Stiffness of Elliptical Leaf Spring Antivibration Mounts

[Leblouba Moussa, Muhammad Ekhlasur Rahman]

Abstract—**This paper presents an analytical solution to the in-plane compressive stiffness of elliptical leaf spring anti-vibration mounts (ELS). The accuracy of the proposed solution has been verified with the finite element analysis of the ELS 3D solid model. Parametric analysis conducted to study the effects of transverse shearing, ELS geometry, and compound material properties on the stiffness showed that the transverse shearing has negligible effect and led to the development of useful equations that simplify the determination of the spring stiffness. In addition, it was demonstrated that the stiffness is more sensitive to the outer radius as compared to other design parameters.**

Keywords—**Elliptical leaf spring, anti-vibration mount, spring stiffness**

I.   Introduction

Shock and vibration isolation of sensitive equipment and machinery has become an integrated part of every engineering design. Vibrations may be from a natural source such as earthquakes, or from artificial sources such as those originated from operating machines. Such vibrations may result in equipment failure, structural damages, or human injuries, depending on the severity of the disturbing vibrations and the sensitivity of the equipment/facility.

Tse and Lung (2000) carried out finite element analysis and theoretical study on large deflections of composite circular springs and validated their results by experiments under uniaxial tension. The authors found that the spring stiffness increased with deflection and hard spring behavior was observed for the whole range of applied loads. The shear and longitudinal deformations effects were found to be negligible for configurations in which the elastic modulus to shear modulus ratios were not large and the radius to thickness ratios were large. In another study, Tse et al. (2002) considered the case of composite circular springs with extended flat contact surfaces and carried out finite element analysis and theoretical study on the new spring stiffness under unidirectional line loading and surface loading configurations.

Leblouba Moussa
High National School of Public Works, Algiers
Algeria

Muhammad Ekhlasur Rahman
School of Engineering and Science/Curtin University Malaysia Campus
Malaysia

The authors showed that the spring stiffness increases with the increase in width and thickness of the composite spring but decreases with the increase in inner radius. However, the spring stiffnesses were more sensitive to the change in spring radius than the thickness.

Advanced Antivibration Components (AAC, Inc.) developed a series of shock and vibration mounts known as elliptical leaf spring antivibration mounts (Fig. 1). Their basic design employs two or more high range of tensile stainless steel ”U” formed leaves, situated at each end, forming an elliptical shape when joined together in the center portion with face plates. The spaces between the ”U” formed leaves are filled with a specially developed polymer (X-mounts) or stainless steel mesh (XM-mounts). The elliptical leaf spring mounting (ELS) was specifically designed for shipboard applications and is particularly suitable to protect marine equipment from shock due to underwater explosions. Later, the ELS application has been extended to isolate heavy machinery, air compressors, engine suspensions, sensitive equipment, etc. Features of the ELS mounts include the effective operation at at low natural frequency and ability to attenuate large shock inputs (Chan et al., 1995)

The main objective of this investigation is to study the in-plane vertical compressive stiffness of ELS mounts with and without damping compound (Fig. 1). Analytical solution is developed for the case of ELS without compound, this solution is based on Castigliano's theorem. For the case of ELS with compound of different material properties, analytical solution is developed based on a statistical analysis of data generated from parametric finite element analysis of the ELS three-dimensional solid models.

Figure 1.   3D view of the ELS mount

II. Analytical Solution

Fig. 2 depicts one quarter of an ELS mount, the spring consists of two flat surfaces (I and II), one elliptic portion with outer radius "R_e" from center "c" and internal radius "Ro" from point "o" (IV), one semi-circular portion with mean radius ($R_e - t/2$) from center c (V), and a flat tapered portion (III) connecting portions II and IV, the upper surface of portion III is flat and the bottom surface is circular with radius "R_o" from point "o". With reference to Fig. 2, the following are the geometric features of the ELS mounts: $R_o = R_e + 0.8t$, β=1.44, ρ= 0.28, γ=36.8°, and $h_f = 0.05$ in (1.27 mm).

In the development of the analytical solution to the ELS stiffness we consider the compound as if it is made of the same material of the leaves, E_f (without compound case, $E_c = E_f = E$). The ELS is subjected to the action of two equal and opposite line loads P acting along the vertical diameter of the spring (Fig. 3(a)). Since the radius of curvature of the spring is large enough than the thickness t, then the stress distribution across the thickness of the spring varies linearly, hence, in applying Castigliano's theorem, the complement energy of flexure due to bending can be considered with sufficient accuracy. Due to symmetry, only one quadrant of the ELS need to be considered (Fig. 3(b)). The bending moment M_0 acting on the A-A cross section makes the system statically indeterminate. This moment can be calculated using Castigliano's theorem. Since the rotation δϕ corresponding to M_0 is zero, we have

$$d\digamma = dU/dM_0 = 0 \qquad (1)$$

in which U is the strain energy due to bending of the quadrant of the spring under consideration.

To simplify the solution steps we divide the considered spring quadrant into five parts (Fig. 2), where the total strain energy, U will be the sum of all energies contributed by each part, that is:

$$U = U_I + U_I + U_{III} + U_{IV} + U_V \qquad (2)$$

Part I, [0, L1]: The strain energy contributed by this part is:

$$U_I = \int_0^{L1} \left[(M_I(x))^2 / 2EI_1 \right] dx \qquad (3)$$

where

$$M_I(X) = P(X) - M_0 \qquad (4)$$

is the bending moment at distance x from the right face of part I, and:

$$I_I = Bt_0^3/12 \qquad (5)$$

is the second moment of inertia of the section at any distance x from the right face of part I.

Part II, [L1, L]: The strain energy contributed by this part is:

$$U_{II} = \int_0^{L2} \left[(M_2(x))^2 / 2EI_2 \right] dx \qquad (6)$$

where the bending moment at distance x from the right face of part II is:

$$M_2(X) = P(L1 + X) - M_0 \qquad (7)$$

and the second moment of inertia

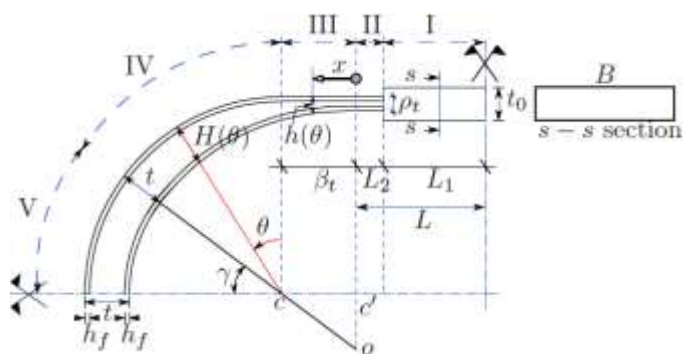$$I_2 = B(\ulcorner t)^3/12 \qquad (8)$$

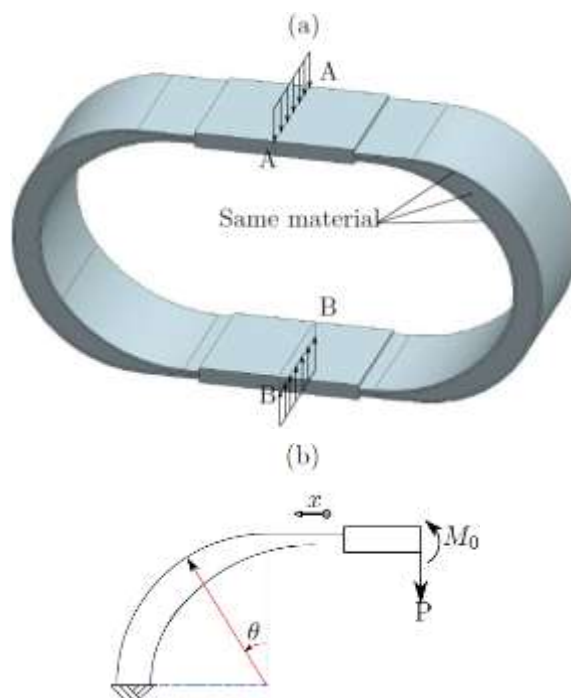Figure 2. Geometry of the ELS mount

Figure 3. ELS mount under compressive loads and its equivalent quadrant

Part III, [L, L + β t]: The strain energy contributed by this part is:

$$U_{III} = \int_0^{bt} \left[(M_3(x))^3 / 2EI_3 \right] dx \qquad (9)$$

where

$$M_3(x) = P(L + x) - M_0 \qquad (10)$$

and

$$I_3(X) = B(h(x))^3 / 12 \qquad (11)$$

h(x) is the thickness of the tapered part (see Fig. 2), it is a function of the distance x starting from the right face of this part:

$$h(x) = \Gamma t + R_0 - \sqrt{R_0^2 - x^2} \qquad (12)$$

Part IV : θ in [0,π/2-γ]: The strain energy contributed by this part is:

$$U_{IV} = \int_0^{P/2-g} \left[(M_4(q))^3 / 2EI_4 \right] r dq \qquad (13)$$

where

$$M_4(q) = P(L + bt) + P\sin(q)(R_e - Hq/2) - M_0 \qquad (14)$$

and

$$I_4(q) = B(h(q))^3 / 12 \qquad (15)$$

H(θ) is the thickness of this part, it is a function of the angle θ (see Fig. 2):

$$H(q) = Re - \sqrt{S^2 + R_0^2 - 2SR_0 \sin[\arcsin(\frac{S\cos(q+g)}{R_0} + q + g)]} \qquad (16)$$

where

$$S = R_o - R_e + t \qquad (17)$$

Part V, θ in [π/2-γ, π/2]: The strain energy contributed by this part is:

$$U_{IV} = \int_{P/2-g}^{P/2} \left[(M_5(q))^3 / 2EI_5 \right) (R_e - t/2) \right] dq \qquad (18)$$

where

$$M_5(q) = M_4(\frac{P}{2} - g) + P[\sin(q)(Re - \frac{t}{2}) - \sin(\frac{P}{2} - g)(Re - \frac{H(\frac{P}{2} - g)}{2})] \qquad (19)$$

and

$$I_5(q) = Bt^3 / 12 \qquad (20)$$

At this stage the bending moment M_0 can be calculated from Eq.1 then substituted back into the strain energy expression (equation (2)) to calculate the vertical deflection, δv:

$$dv = \P U / \P P \qquad (21)$$

The in-plane compressive stiffness, k_v is then:

$$k_v = P / dv \qquad (22)$$

III. Numerical Analysis

Finite element predictions of the vertical deflection of several ELS mounts were carried out. The antivibration mounts are made of stainless steel leaves (E_f = 200 GPa, v_f = 0.3). The outer and inner "U" shaped leaves, having constant thickness h_f = 0.05 in (1.27 mm), are riveted together at the open ends with face plates to form an elliptical shaped assembly. The space between the stainless steel leaves is filled with a polymer (epoxy resin in general) damping compound.

Table 1 summarizes the geometric properties of the ELS mounts considered in this study. The width B of the springs is varied from 0.5 in (12.7 mm) until 4 in (101.6 mm). The elastic modulus of the compound material is varied to cover a wide range of possible filling: from E_c = 3 GPa (e.g., epoxy resin) until E_c = E_f (stainless steel filling or no compound). Poisson's ratio of the compound material is found to have negligible effect on the vertical deflection of the spring, thus, it is kept constant at v_c = v_f.

TABLE I.   GEOMETRY OF THE SELECTED ELS MOUNTS

ELS#	Re(mm)	t (mm)	L1 mm)	L2(mm)	t0 (mm)
ELS1	43.43	11.91	30.48	10.79	6.20
ELS2	52.07	11.91	32.38	6.35	6.20
ELS3	76.83	19.85	44.58	0.0	10.31
ELS4	32.89	9.21	20.04	3.71	5.40

Finite elements defined by 20 nodes having 3 degrees of freedom per node are employed in the FEA. This type of element can tolerate irregular shapes and is capable to model

curved boundaries. Only linear analysis is employed for this study. All nodes along the line B-B at the bottom were fixed. Nodes along the line A-A at the top were subjected to a line-loading and were constrained in the out-of-plane directions.

IV. Results & Discussion

The compressive stiffnesses obtained by theory and finite element analysis are listed in Table 2 for the case of $E_c = E_f$. It is observed that there is good agreements between theoretical and numerical results. However, small discrepancies of about 6.2% are noted at relatively high stiffness where the spring width is the largest. Note that the transverse shearing effects are insignificant in these cases.

Fig. 4 shows the stiffness-width relationship of the ELS mounts. In this study, the ELS width was varied from 0.5 in (12.7 mm) to 4 in (101.6 mm), while the remaining design parameters were kept constant. The stiffnesses of all ELS mounts increase linearly with the increase in spring width, B. Evidently, the ELS mounts with stainless steel compounds ($E_c = E_f$) are stiffer, however, the rate of change in their stiffness is higher than the springs with softer compound materials (i.e., $E_c < E_f$). Fig. 5 plots the variation of ELS stiffness with the outer radius, R_e. In this study, the outer radius was varied from 1.2 in (30.48 mm) to 4 in (101.6 mm) and the dependent parameter, R_o, was updated accordingly; $R_o = R_e + 0.8t$, while the remaining parameters were kept constant. It is observed that an increase in the outer radius decreases the spring stiffness; an increase in the outer radius induces a quadratic decrease of the spring stiffness.

To study the effect of spring length on the compressive stiffness, the lengths L_1 of the face plate (total face plate length is $2 L_1$) and L_2 of the extended flat surface were varied to cover a wide range of practical ELS mounts and the stiffness was recorded for every pair (L_1, L_2), the results are reported in Fig. 6. In this investigation, all parameters were held constant except for the pair (L_1, L_2). It is clear that the ELS stiffness is highly dependent on the length of the flat surfaces. For short L_2, an increase in L_1 reduces slowly the spring stiffness, and for long L_2, an increase in L_1 has little effect on the stiffness. However, for short L_1, an increase in L_2 significantly reduces the spring compressive stiffness, but for long L_1, an increase in L_2 reduces the stiffness with a small rate (up to 1/4). When $L_2 = 0$, slight increase in L_1 reduces considerably the stiffness.

The analytical solution of the stiffness developed in section 3 deals only with the case of ELS mounts made of a single material. In addition, it is difficult to find an analytical solution to the case of ELS with a compound made of different material properties. However, the proposed analytical solution may still be useful to obtain empirical equations to the stiffness of ELS mounts with a compound made of a material different of that of the leaves. For this, a statistical analysis would be needed.

Table 2 shows that the error in estimating the ELS stiffness increases with the width B, this is due to the fact that the analytical solution accounts only for bending effects.

TABLE II. THEORETICAL AND NUMERICAL ELS STIFFNESS ($E_c = E_F$)

| ELS#	B (mm)	Theoritical (N/mm)	Numerical (N/mm)	Error (%)
ELS1	25.4	2146.38	2124.36	1.04
	50.8	4292.76	4361.29	-1.57
	76.2	6439.13	6693.00	-3.79
	101.6	8585.51	9060.43	-5.24
ELS2	25.4	1893.54	1878.36	0.81
	50.8	3787.09	3848.38	1.59
	76.2	5680.62	5911.91	-3.91
	101.6	7574.04	8001.92	-5.35
ELS3	25.4	3517.37	3581.53	-1.79
	50.8	7034.75	7253.74	-3.02
	76.2	10552.12	11066.35	-4.65
	101.6	14069.50	15005.10	-6.24
ELS4	25.4	4464.75	4447.01	0.40
	50.8	8929.51	9226.79	-3.22
	76.2	13394.26	14121.70	-5.15
	101.6	17859.01	18974.25	-5.88
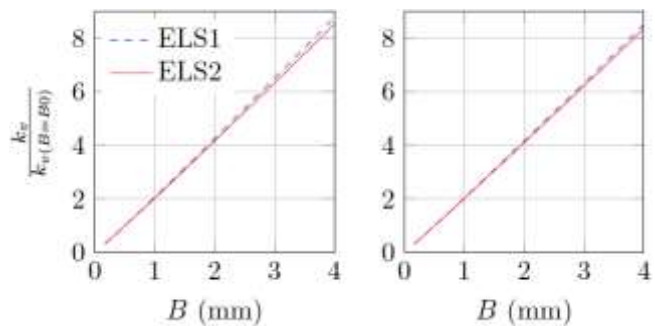
Figure 4. Variation of the stiffness with spring width (Bo=12.7mm)
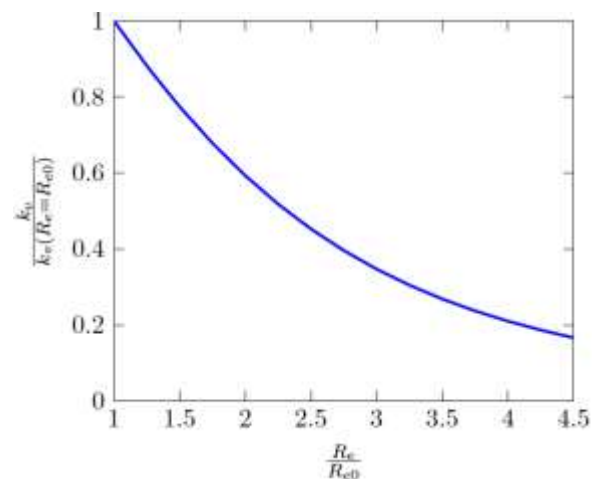

Figure 5. Variation of the ELS stiffness with outer radius

Fig. 7 shows the variation of the normalized spring stiffness ($k_v/k_v(E_c = E_f)$) with the variation of the factor $n_E = E_c/E_f$. The normalized stiffness increases with the compound material young's modulus, E_c, and this variation is independent of the spring width, B. Shown in the same figure is the equation that fits the variation curve, which is:

$$K_v @ K_v, n_E = \left[0.765 + 0.259 n_E - 0.0221 \middle/ \sqrt{n_E}\right] \qquad (23)$$

Even though in the analytical solution the error in estimating the ELS stiffness increases with the spring width, the analytical stiffness is still useful because the stiffness varies linearly with the spring width (Fig. 4).
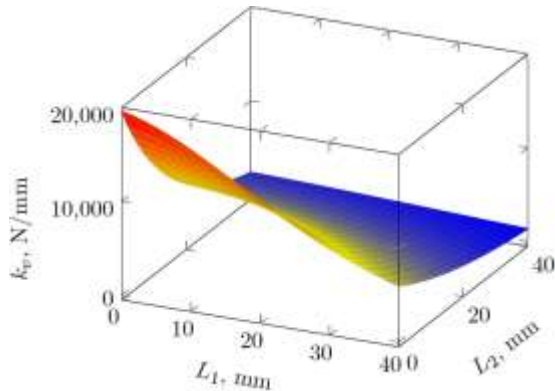

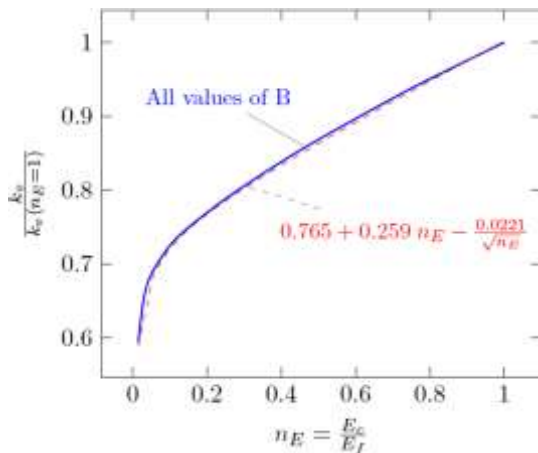Figure 6.   Effect of the L1 and L2 on the stiffness of an ELS mount

Figure 7.   Variation of ELS normalized stiffness with n_E

Fig. 8 shows the variation of the normalized stiffness $(k_v/k_v(B = B_0))$ with the variation of the factor $n_B = B/B_0$, where B_0 is chosen to be equal to 0.5 in (12.7 mm). It is clear that n_E factor has negligible effect on the variation of the normalized stiffness. From the analytical solution, which is valid only for the $n_E = 1$, that variation of the normalized stiffness is exactly linear and is equal to n_B, however, from the numerical solution, which takes into account almost all possible effects, the variation of stiffness follows the power trend:

$$K_v \middle/ Kv_{n_E=1}^{n_B=1} @ 0.989 n_B^{1.036} @ n_B^{1.036} \qquad (24)$$

Combining equations (23) and (24) yields:

$$K_v @ K_{n_E=1}^{n_B=1} n_B^{1.036} = \left[0.757 + 0.256 n_E - 0.022 \middle/ \sqrt{n_E}\right] \qquad (25)$$
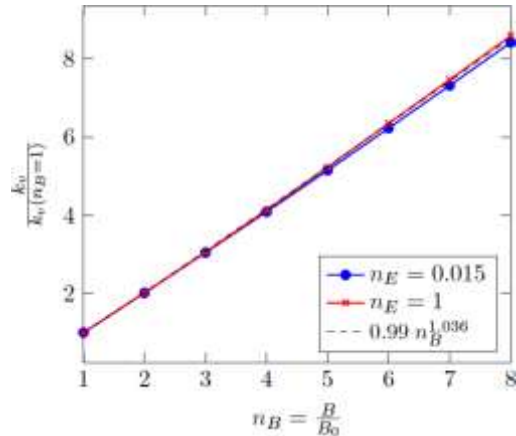

Figure 8.   Variation of ELS normalized stiffness with n_B

To avoid running FEA of complete 3D ELS solid models, the analytical stiffness provided by equation (22) can be used to calculate the stiffness of the spring with $n_E = 1$ (i.e., $E_c = E_f$) and $n_B = 1$ (i.e., any width $B = B_0$), and by injecting the obtained value in equation (25) one can determine with sufficient accuracy the stiffness of the ELS with a compound of different material ($n_E \neq 1$) and different width ($B \neq B_0$).

V.   Conclusion

In this paper theoretical and numerical analyses on the in-plane compressive stiffness of Elliptical Leaf Spring antivibration mounts under line-loading have been studied. The investigation led to the following conclusions:

1. The transverse shear included implicitly in the three-dimensional finite element analysis was found to have a negligible effect for practical design parameters.
2. The compressive stiffness increases with the spring width and decreases with the outer radius, the face plate and extended flat surface lengths. Within practical values of face plate length, the ELS stiffness reduces with the increase of the extended flat surface length;
3. The spring stiffness is more sensitive to the outer-radius; doubling the outer radius decreases the stiffness more than three times, while doubling the length of the face plate reduces the stiffness up to a maximum of three times.
4. In this study we developed a set of equations for the determination of the in-plane compressive stiffness of ELS mounts based on theoretical and numerical investigations.

Acknowledgment

References

[1] G. Eason, B. Noble, and I. N. Sneddon, "On certain integrals of Lipschitz-Hankel type involving products of Bessel functions," Phil. Trans. Roy. Soc. London, vol. A247, pp. 529–551, April 1955. *(references)*

[2] Tse, PC and Lung, TC, "Large deflections of elastic composite circular springs under uniaxial tension," Int. J. Nonlinear Mech. Elsevier, vol. 35, pp. 293-307, 2000.

Tse, PC and Lau, KJ and Wong, WH and Reid, SR, "Spring Stiffnesses of composite circular springs with extended flat contact surfaces under uniderctional line-loading and surface-loading configurations," Compos. Struct. Elsevier, vol55, pp. 367-386, 2002.

[3] Yew Wing Chan, S. Olutunde Oyadiji, Geoffrey R. Tomlinson and J. R. Wright, "Predicting the vibration characteristics of elements incorporating incompressible and compressible viscoelastic materials," Proc. SPIE 2445, Smart Structures and Materials, 1995[Passive Damping, 293, May 5, 1995].

About Author (s):

	Dr. Leblouba Moussa is currently an Assistant Professor of Civil Engineering with the High National School of Public Works (ENSTP) of Algiers, Algeria.
	Dr. Muhammad Ekhlasur Rahman is currently a Senior Lecturer of Civil Engineering with Curtin University Sarawak Campus, Malaysia.